Formation and morphology of InAs/GaAs heterointerfaces

O. Brandt, K. Ploog,* and L. Tapfer†
Max-Planck-Institut für Festkörperforschung, Heisenbergstrasse 1, D-7000 Stuttgart 80, Germany

M. Hohenstein, R. Bierwolf, and F. Phillipp
Max-Planck-Institut für Metallforschung, Heisenbergstrasse 1, D-7000 Stuttgart 80, Germany
(Received 23 April 1991; revised manuscript received 5 August 1991)

The synthesis of perfect InAs/GaAs heterostructures by conventional solid-source molecular-beam epitaxy is achieved by a growth approach that employs the modulation of growth temperature during the interface formation. Details of the evolution of the growth front during interface formation are probed by *in situ* reflection high-energy electron diffraction. The nucleation of InAs on GaAs occurs layer by layer for the first two monolayers. At this stage, the InAs film wets the underlying GaAs; i.e., a continuous coverage of the substrate is thermodynamically preferred. Thus, allowing the growth front to relax towards the equilibrium state minimizes the step density on the surface. During overgrowth of the InAs film with GaAs, a fraction of the deposited In segregates on the growing surface. This In floating layer is desorbed prior to overgrowth by a heating cycle, which prevents its incorporation into the GaAs capping layer. The resulting exceptional degree of crystalline perfection of the InAs/GaAs heterostructures is confirmed by double-crystal x-ray diffraction patterns of multilayer structures which are essentially indistinguishable from the theoretical pattern predicted by the dynamical diffraction theory. The atomic configuration at the InAs/GaAs interfaces is studied by high-resolution electron microscopy. Extensive image simulations provide reliable quantitative information on layer thickness and interface configuration. Lattice images of InAs films having thickness in excess of two monolayers reveal that both interfaces are structurally equivalent. Fluctuations of the interfaces are restricted to monoatomic steps. The atomic-scale morphology of these highly strained interfaces compares favorably with that of GaAs/$Al_xGa_{1-x}As$ heterointerfaces. The crucial point for obtaining this structural perfection is the flashoff of the In floating layer prior to GaAs overgrowth.

I. INTRODUCTION

Molecular-beam epitaxy (MBE) nowadays routinely demonstrates its capability of controlling the growth of semiconductor heterostructures down to the atomic scale.[1] The synthesis of multilayer structures with an arbitrary combination of the constituent materials is, however, beset with several fundamental problems.[2,3] The fabrication of an embedded layer requires first the deposition of an epilayer A on the underlying substrate B, followed by the capping layer of the substrate material. At sufficiently high temperatures allowing epitaxial growth, however, the deposited film can attain a thermodynamically stable state, determined by the combination of surface- and interface-free energies.[4–7] For only one of the two materials, the specific energetics do favor wetting of the underlying layer; i.e., either material A or B nucleates via immediate islanding (Volmer-Weber mode). In addition, even if the overlayer wets the substrate, the overlayer strain may induce a morphological phase transition from layer-by-layer growth to islanding (Stranski-Krastanov mode), allowing the overlayer to lower its total energy by nucleation of dislocations at the island edges.[5,8]

The system InAs/GaAs represents a particularly challenging candidate for the study of heteroepitaxial growth. The lattice mismatch between InAs and GaAs is 7.16%. The growth of InAs on (001) GaAs is layer by layer for the first two monolayers (ML), while island formation and strain relief occurs thereafter.[9,10] Since the InAs overlayer wets the underlying GaAs, the balance of surface and interface energy dictates an immediate islanding of subsequent GaAs on top of an InAs film. Any attempt to form an InAs film embedded within GaAs layers has to overcome this fundamental limitation imposed by the thermodynamics of the growth process. Besides these thermodynamic restrictions, kinetic processes during growth may additionally participate in the interface formation. In fact, when overgrowing InAs with GaAs there is significant segregation of In atoms on the growth surface.[11–13] *In situ* surface-analytical techniques like Auger electron spectroscopy and x-ray photoemission spectroscopy have provided important insight into this segregation process. A buildup of In on the surface is detected during overgrowth of InAs films, which is phenomenologically ascribed to atomic-exchange reactions between In and Ga atoms at the growth front. The In atoms thereby form a quasiliquid phase on the growing crystal,[14] the so-called In floating layer. The floating layer is gradually dissolved during subsequent overgrowth, preventing the formation of a well-defined abrupt InAs/GaAs interface.[11,15] The segregation process has been found to be independent both of temperature and of the arriving fluxes; i.e., it cannot be controlled by growth parameters. This finding has led to the conclusion that segregation is an inherent property of the GaAs/InAs

 ©1992 The American Physical Society

heterointerface, causing any attempt at interface control to fail.[12,16]

In this work, we study the formation and the structural configuration of InAs/GaAs heterointerfaces, which are synthesized by a modified growth procedure based on conventional solid-source MBE. Reflection high-energy electron diffraction (RHEED) provides direct insight into the evolution of the growth front while interface formation occurs. The morphology of the resulting heterointerfaces is investigated by high-resolution double-crystal x-ray diffractometry (HRDXD) and high-resolution electron microscopy (HREM). The experimental results are analyzed within the adequate theoretical framework to obtain reliable quantitative information on layer thickness and interface morphology. The important result of the use of optimized growth conditions is that both InAs/GaAs and GaAs/InAs interfaces are of equivalent abruptness and neither a compositional gradient nor short-range roughness exists at either of the interfaces. The reason for this surprising structural perfection is the flashoff of the In floating layer prior to GaAs overgrowth.

The paper is organized as follows. In Sec. II, we first describe the experimental setup used for our investigations. In Sec. III, we outline the essential characteristics of our growth technique, and report on RHEED experiments during the formation of the interfaces. In Sec. IV, we present the x-ray diffraction patterns of InAs/GaAs heterostructures and discuss their analysis by the dynamical diffraction theory. In Sec. V, the results of HREM experiments are presented and interpreted. Finally, in Sec. VI, we summarize the results and draw our conclusions.

II. EXPERIMENTAL SETUP

The samples are synthesized in a three-vacuum-chamber MBE system, equipped with elemental solid sources providing atomic species of Ga and In and tetrametric As_4 molecules. They are deposited on exactly (001)-oriented ($<0.1°$ off) undoped (semi-insulating) GaAs substrates mounted In free on a molybdenum holder. Both the effective substrate temperature and the net fluxes on the surface are calibrated *in situ* by means of RHEED, using a 30-keV electron gun operating at a glancing-incidence angle of 1°. The RHEED patterns are recorded with a video camera connected to an image-processing system. The temperatures mentioned in the present work refer to the evaporation of the native oxide at 580 °C (Refs. 17 and 18) and the transition from the As-stabilized to the Ga-stabilized regime at 630 °C,[19] as observed by monitoring the RHEED pattern during the substrate preparation. The Ga arrival flux (deposition rate) is set to 1 ML/s by monitoring RHEED-intensity oscillations during the buffer layer growth. One-monolayer GaAs refers to the complete coverage of the (100) surface with Ga and corresponds to 6.24×10^{14} cm^{-2} Ga atoms. An As_4/Ga ratio of about 1 is established as calibrated by arsenic-induced RHEED-intensity oscillations[20] in previous growth runs. The deposition rates for InAs are determined precisely by HRDXD and compared to those obtained by scanning electron micrographs from cleaved edges of bulk-InAs layers.[21] The In and As_4 arrival fluxes used correspond to a deposition rate of 1 ML InAs per 16 s and an As_4/In ratio close to the stoichiometric minimum. Here, one monolayer In refers to the complete coverage of the (100) surface with In, corresponding to the same number of atoms as for Ga (6.24×10^{14} cm^{-2}), if the In atoms are in registry with the underlying lattice.

The x-ray measurements are performed by using a computer-controlled double-crystal x-ray diffractometer operating in the nondispersive Bragg geometry.[22] A rotating-anode 12-kW generator with a copper target ($\lambda_{Cu\ K\alpha_1}=0.1540562$ nm) is employed as the x-ray source. A well-collimated monochromatic x-ray beam is obtained by using an asymmetrically cut (100) Ge crystal and the (400) reflection. The size of the x-ray beam incident on the specimen crystal is 0.2×1.5 mm^2, and its angular divergence is 11 μrad. This value is much smaller than the intrinsic width of the (004) GaAs reflection, allowing us to neglect the convolution with the monochromator response function.

For the HREM experiments, cross-sectional samples along the [110] direction are prepared by conventional ion milling. The specimen thickness is then 12 nm. Lattice images are taken in a JEOL-JEM 4000FX electron microscope operating at 400 kV. The micrographs are recorded with untilted illumination and the objective aperture being centered around the direct beam. Spatial frequencies up to 6 nm^{-1} are transmitted. The defocus value is -20 nm. For image processing the micrographs are digitized using a EIKONIX camera.

III. FORMATION OF THE InAs/GaAs HETEROINTERFACE

Prior to the deposition of the InAs/GaAs structure, a 1-μm-thick GaAs buffer layer is grown at 580 °C. The GaAs surface is then annealed for 2 min at the same temperature. The (2×4) RHEED pattern of the static GaAs surface recorded with the electron beam along the $[1\bar{1}0]$ direction exhibits sharp elongated diffraction spots lying on the zeroth-order Laue zone. This diffraction pattern is characteristic of the most ordered surface possible under the (2×4) reconstruction.[23,24] Thus, the maximum surface smoothness is ensured for deposition of the subsequent InAs/GaAs heterostructure.

In Fig. 1, we present a scheme of the growth procedure for the fabrication of a single InAs/GaAs heterointerface. The GaAs layers embedding each InAs film are grown at 540 °C. To initiate InAs deposition, the temperature is lowered to 420 °C. Then the InAs layer is deposited in 0.6-ML increments, annealing the growth surface after each deposition under As_4 for 120 s at the growth temperature of 420 °C. Before heating up again to 540 °C for GaAs overgrowth, 3 ML of GaAs are deposited at 420 °C on top on the InAs layer. We note that the thickness of this intermediate layer turned out to be an essential parameter for the structure, as will be discussed below. Then growth is stopped and the temperature is raised to the growth temperature of GaAs (540 °C) before GaAs growth is continued.

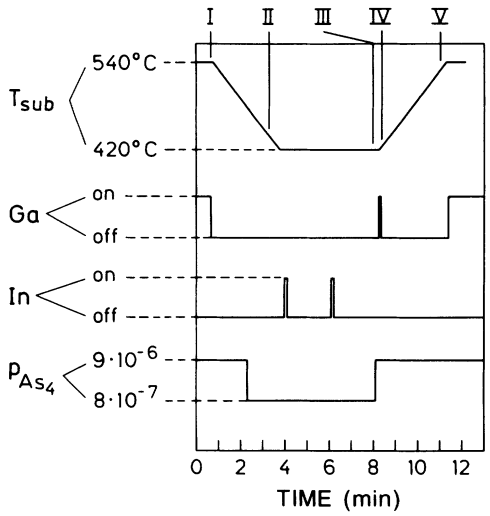

FIG. 1. Schematic diagram of the temperature- and flux-switching procedure during the deposition of 1-ML InAs on GaAs and subsequent overgrowth with GaAs. On the bottom, the deposition time is displayed. In the upper trace, the variation in substrate temperature over time is shown. Roman numbers refer to RHEED patterns taken during the interface formation as presented in Fig. 2. The layer sequence is apparent from the states of the Ga and In shutters, depicted in the two middle traces. First, the In shutter is open two times for 8 s each for deposition of 0.6-ML InAs. After the InAs increments the surface is annealed for 120 s. Then the Ga shutter is open one time for 3 s to deposit 3-ML GaAs. In the lower trace, the beam equivalent pressure of the As_4 flux impinging on the surface is displayed.

During this procedure, the growth process is monitored by RHEED as indicated by the roman numbers in Fig. 1. The corresponding RHEED patterns are shown in Fig. 2. When the temperature is lowered for InAs growth, the (2×4) reconstruction of GaAs (I) changes to the $c(4\times4)$ reconstruction (II), originating from excess As_4 sticking on the surface.[25] After opening of the In shutter for the first 0.6 ML, a (2×3) reconstruction with diffuse half-order streaks appears. After the second In supply, the reconstruction streaks first disappear, but develop again while growth is stopped (III). The nature of this reconstruction and the role of the annealing cycle are addressed in Sec. III A. When the Ga shutter is opened, the reconstruction disappears and a (1×1) pattern is observed (IV). Finally, during the subsequent heating to 540 °C, a well-defined $(2\times4)_\gamma$ reconstruction[26] appears at 520 °C (V). This change in reconstruction directly reflects the flashoff of the In floating layer on the surface, as will be discussed in detail in Sec. III B.

A. Nucleation of InAs on GaAs

The (2×3) reconstruction observed during the InAs growth corresponds to As_4-stable conditions,[10,27] despite the fact that the actual $[As_4]/[In]$ ratio corresponds to In-stable conditions during bulk growth [a (4×2) reconstruction is observed under these experimental conditions after the deposition of about ≃1000 Å InAs]. We thus attribute this finding to the presence of excess As_4 adsorbed on the GaAs surface at temperatures below ≃450 °C, which acts as the source of As for termination of InAs rather than the impinging flux. In contrast to the case of bulk InAs,[9] the quality of these ultrathin strained films is not affected by the presence of excess As_4. Probably the long annealing cycles relax the restriction of accurate control of the effective-surface stoichiometry.

The employed annealing cycles have another important

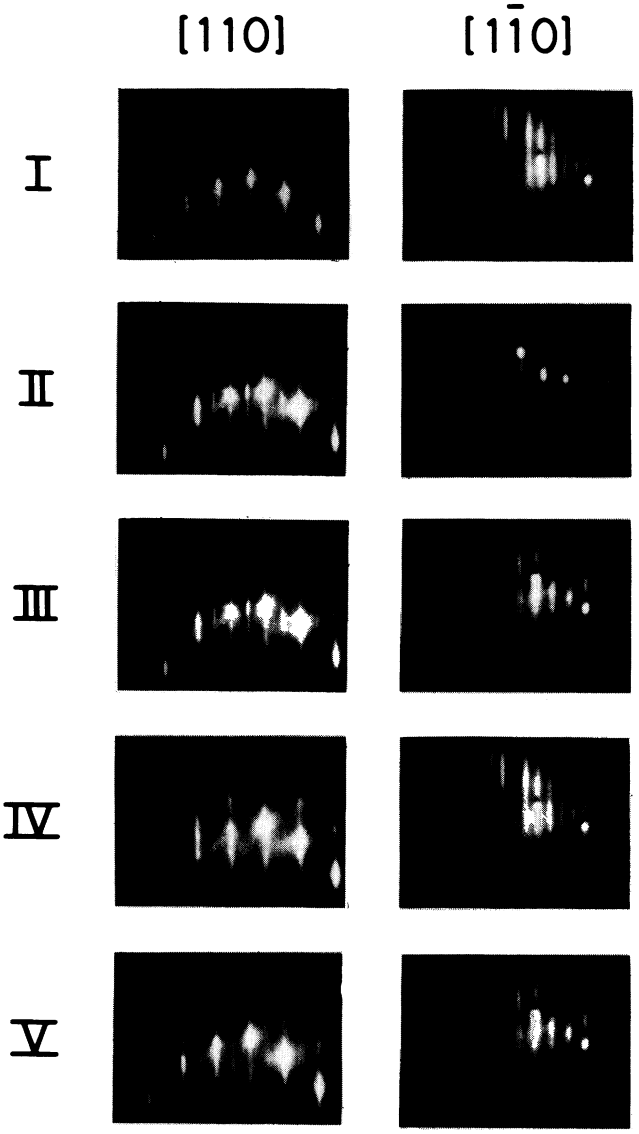

FIG. 2. RHEED patterns taken during the deposition of 1.2-ML InAs on GaAs and the subsequent overgrowth with GaAs. Roman numbers refer to Fig. 1. The azimuth of the incident electron beam is denoted on the top. (I) (2×4) reconstruction of the dynamic (growing) GaAs surface at 540 °C, (II) $c(4\times4)$ reconstruction of the static (nongrowing) GaAs surface at 440 °C, (III) (2×3) As-stable reconstruction of the static InAs surface after deposition of ≃1.2-ML InAs at 420 °C, (IV) (1×1) reconstruction of the static surface after deposition of ≃3-ML GaAs at 420 °C on top of the InAs monolayer, (V) $(2\times4)_\gamma$ reconstruction of the same (static) surface at 520 °C.

consequence. The fractional-order streaks of the InAs reconstruction are not present during the deposition, but develop during the annealing. This temporal evolution of the reconstruction reflects the dynamic recovery of the surface toward an equilibrium state,[28–30] and is most evident when growing InAs layers with a thickness close to the onset of three-dimensional nucleation. In Fig. 3, we display the RHEED patterns taken from the recovering InAs surface after six deposition steps, i.e., the deposition of 3.6-ML InAs, and at different times after closing the In shutter. This structure has been examined by HRDXD (see Sec. IV) and, in addition, by double-crystal x-ray topography, and no dislocations are detected by either of these techniques. The pattern at $t=0$ corresponds to the surface when deposition is just completed. At this stage, the reconstruction streaks are considerably broadened, revealing an increasing roughness developed on the growing surface. Furthermore, an intensity modulation along the streak direction can be seen. This observation clearly indicates the onset of islanding, i.e., the change from layer-by-layer growth to three-dimensional nucleation as a consequence of the Stranski-Krastanov growth mode of InAs on GaAs. The pattern obtained after 60 s reveals a return to a smooth [(two-dimensional) (2D)] growth front. After 120 s, the reconstruction is similar to that shown in Fig. 2 for only 1.2 ML InAs (pattern III). Hence, the surface recovery is quite effective and leads to a well-ordered surface.

The nature of the recovery process is elucidated by the observation that no surface recovery occurs after eight deposition steps, i.e., after the deposition of 4.8-ML InAs.[31] Then the fractional-order streaks are replaced by V-shaped features around sharp diffraction spots, indicating strong faceting on the surface. The pattern remains unchanged even after 30-min annealing. HREM examination of InAs films of this thickness reveals the presence of two types of 60° dislocations at the island edges, with their Burgers vectors inclined on opposing {111} planes.[31] Hence the recovery process is intimately related to the strain state of the film which, in fact, is consistent with the general principles of heteroepitaxial growth. For materials growing in the Stranski-Krastanov mode, nucleation occurs layer by layer in the first stage of growth. Thus a continuous (two-dimensional) coverage of the surface is energetically preferred. Allowing the surface to relax toward equilibrium then leads to the dissociation of spontaneously formed islands and the subsequent incorporation of migrating In adatoms into energetically more favorable sites, e.g., kinks in monolayer step edges.[32,33] However, a morphological phase transition, induced by the buildup of strain in the overlayer, occurs after the deposition of a certain amount of material. At this thickness, an agglomerated (three-dimensional) morphology is energetically preferred, and the surface recovery will favor cluster formation. One should bear in mind that this change in morphology may or may not be accompanied by the formation of dislocations.[7] In the particular case of InAs on GaAs, the formation of islands exceeding a critical volume in fact initiates the nucleation of dislocations at island edges.[31]

Attempts to prevent the morphological phase transition and thereby to maintain two-dimensional films have to adopt an opposite strategy to that applied here. Films which are metastable with respect to the morphological phase transition may be realized by driving the system far away from equilibrium, i.e., by preventing surface relaxation using high deposition rates and low temperatures.[3,6] This approach may bypass severe agglomeration, but in any case the resulting films will exhibit considerable roughness on an atomic scale. Thus, abrupt interfaces can be realized when the two-dimensional surface coverage is thermodynamically favored, but not when the growth front is just kinetically limited.

B. Overgrowth of InAs by GaAs

The (1×1) RHEED pattern observed in the first stage of overgrowth (IV) is in striking contrast to the $c(4\times4)$ reconstruction usually observed for the GaAs surface at this temperature and As_4 flux (II). However, the appearance of long diffraction streaks demonstrate that islanding of GaAs on InAs is prevented. The use of a low growth temperature (420 °C) and a high deposition rate (1 ML/s) thus imposes kinetic limitations on the film morphology, inhibiting relaxation to the equilibrium

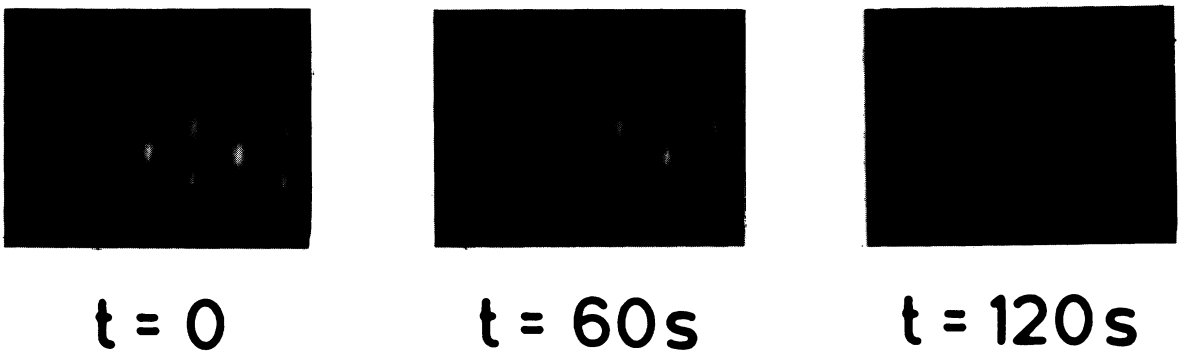

FIG. 3. RHEED patterns of the relaxing InAs surface taken along the [110] azimuth after the deposition of 3.6-ML InAs (six deposition steps) on GaAs at 420 °C. The time indicated at the respective pattern corresponds to the annealing time after closing the In shutter.

configuration (agglomerated morphology). Instead, the lack of surface reconstruction indicates the presence of a surface-active species on the growth surface. In particular, a (1×1) reconstruction is frequently observed when growing $Al_xGa_{1-x}As$ in the so-called forbidden temperature range, where a Ga floating layer is present at the surface.[34,35,14]

Our experimental finding thus suggests the existence of an In floating layer on the surface. The subsequent heating to 540 °C leads to the formation of a well-defined (2×4) reconstruction at 520 °C (V). Both elementary In on GaAs and InAs on the GaAs start to desorb at around 500 °C.[9,36] The rearrangement of the surface during the heating cycle thus indicates the flashoff of the In floating layer on the surface. This desorption of a fraction of the delivered In should manifest itself in an apparent change of the growth rate. In fact, growth rates derived from the thickness of the embedded InAs films are systematically smaller with respect to those obtained from the equivalent thickness of bulk InAs.[21] Comparing the thickness of InAs films grown with and without the heating cycle provides the direct determination of the amount of In segregating on the surface. Under the growth conditions described above, the thickness of InAs films grown with the heating cycle is about 40% smaller than that of layers grown without, which means that this fraction of In segregates *and* desorbs, thus preventing its incorporation into the subsequent GaAs layer.

Although the flashoff of the In floating layer definitely prevents its incorporation into the GaAs cap layer, In may still be incorporated into the first GaAs monolayers *prior to* flashoff. For continuous overgrowth, standard segregation models actually predict an exponential composition gradient in the cap layer. These models, however, do not apply in the event of interrupted growth, where the system relaxes toward equilibrium. As we are dealing with phase segregation in the presence of a surface, equilibrium here means the separation of surface and bulk phases.[12] The abrupt composition change between bulk and surface phases occurs via the depletion of the subsurface region and the completion of the floating layer. Following these considerations, we attempt to establish surface-subsurface equilibrium by the appropriate choice of duration and temperature of the heating cycle and the thickness of the subsurface region. Since the segregation process is known to be rapid even with respect to the growth rate during MBE, we expect that no kinetic limitations exist for growth interruptions of several minutes. The final temperature of the heating cycle and the thickness of the initial GaAs layer are thus the controlling parameters in our experiments. In fact, both the amount of In lost during the heating cycle and the structural quality of the sample exhibit a systematic dependence on these parameters. For a thickness of 1 ML, the loss of In depends strongly on the final temperature of the heating cycle, and reaches 100% for temperatures above 540 °C. The InAs surface is thus not covered sufficiently to prevent significant desorption of the InAs film itself. For a thickness of 2–3 ML, the loss of In starts at a final temperature of 500 °C and saturates at around 520 °C at 40%. Further heating even above 580 °C does not lead to an increasing loss of In. This observation, together with achieved interface abruptness (see Secs. IV and V), indicates that the employed heating cycle in this case leads to the full depletion of the subsurface region. For a thickness of 5–7 ML, the loss of In is less than that with thinner GaAs layers for the same temperature. Even for final temperatures above 580 °C, the loss of In is only 30%. Simultaneously, a pronounced structural degradation is apparent in the diffraction patterns of these samples. These findings indicate that the surface-subsurface equilibrium is not established for a subsurface depth of much more than 3 ML, or requires impracticable high temperatures during the heating cycle.

The amount of segregated In is found to be, in general, insensitive to the growth conditions, except when Ga and As_4 are supplied alternately ("pulsed") during overgrowth. This technique results in segregation rates up to 90%, determined by the In amount remaining in the final structure. The enhanced segregation rate is also manifested in a clear (2×3) reconstruction after the deposition of 3-ML GaAs, instead of the (1×1) reconstruction observed under continuous fluxes. We ascribe this observation to the formation of a crystalline InAs film on the surface rather than to the presence of an In floating layer, as 90% of the initially deposited amount of In builds up on the growing surface. This finding is consistent with results of other authors making use of the pulsed supply of Ga and As_4 during overgrowth. Yamaguchi and Horikoshi[37] reported a strong asymmetric broadening of the In-concentration profile, extending toward the surface to about 30 nm as detected by secondary-ion mass spectrometry (SIMS). The authors have modeled their observation by a simple phenomenological approach. Assuming that segregation can be described as a replacement of In atoms on the growth surface by subsequently delivered Ga atoms, their experiment suggests an atomic exchange occurring with a probability of 98%. From a practical point of view, growth techniques making use of an alternate supply of Ga and As_4 for overgrowth are thus less suitable for this materials system.

IV. STRUCTURAL ANALYSIS OF ULTRATHIN EMBEDDED InAs LAYERS

High-resolution double-crystal x-ray diffractometry provides accurate information on the structural configuration of semiconductor heterostructures.[22,38] In particular, this technique allows us to detect interface fluctuations on an atomic scale.[39,40] The multiple reflection of phase-coherent x-ray wave fields within perfect heterostructures leads to complex interference phenomena[41–43] (*Pendellösung* fringes). Each constituent layer contributes to the shape of the whole diffraction pattern. Any deviation from structural perfection, i.e., crystalline defects and fluctuations of interfaces and composition, causes the loss of phase coherence of the reflected x-ray wave fields and prevents interference effects. However, the experiment has to be analyzed by an adequate theoretical model to get quantitative information on the interface configuration. To obtain the true phase shift between the interfering x-ray wave fields, the

exact boundary conditions at the heterointerfaces are required; i.e., the dynamical diffraction theory has to be used. In this work, the dynamical diffraction theory for distorted crystals is treated in the recursive formalism.[41,42]

The diffraction experiments are performed (i) on a periodic InAs/GaAs multilayer heterostructure and (ii) on a single InAs layer embedded in GaAs, both fabricated by the procedure described in Sec. III. The thickness of the initial GaAs layer is set in either case to 3 ML. The first of these structures is designed to permit the study of high-order satellite reflections, which are most sensitive to the structural details of the individual interfaces. Ten InAs submonolayer films (0.8 ML) are separated by 31.5-nm GaAs, and a 200-nm GaAs cap layer is deposited on top of the structure. In Fig. 4, we present the (a) experimental and (b) theoretical diffraction pattern in the vicinity of the (400) reflection. For the calculation, the crystal is assumed to be free from defects, having no deviation from structural perfection. Besides the substrate reflection (S), satellite reflections up to the 11th order are observed. The zeroth-order satellite (0) reflects the average properties of the multilayer (mean In content), whereas the higher-order satellites ($\pm m$, $m=1,2,\ldots,11$) originate from the periodic arrangement of the constituent layers. The excellent agreement between the theoretical and experimental satellite line shapes reveals the exact ordering of the layer stacking. In the simulation shown in Fig. 4(b), the lattice constant parallel to the (100) plane is taken to be that of GaAs, i.e., the strain is assumed to be entirely accommodated by an elastic tetragonal distortion of the In-As bond in the [100] direction. This assumption is examined by the diffraction around asymmetric reflections, namely, around (422) and (511). In Fig. 5(a), we show the experimental diffraction pattern recorded in the vicinity of the (422) reflection. The theoretical pattern shown in Fig. 5(b) is calculated with the same set of parameters as that assumed for the symmetric reflection, and it indeed demonstrates the coherently strained state of the InAs layers. It is worth noting that a fractional strain relief of 1% is readily detected thanks to the high resolution of our equipment. To gain quantitative information about the interface fluctuation compatible with the experiment, we compare the experimental and theoretical full width at half maxima (FWHM) of the higher-order satellite reflections. No broadening can be detected even for the highest-order satellite reflections for which the FWHM is still defined (for satellites of order >5 the background intensity is higher than that at half maximum). Since a broadening of about 30 μrad can be resolved, the upper limit for interface fluctuation can be estimated to be 0.1 ML (0.03 nm). The same value has been found in GaAs/AlAs superlattices which are considered to represent the most perfect artificially layered structures.[39] Note, that these experiments do not provide any information about the vertical and lateral scale of the interface fluctuation. This question is consequently tackled by electron microscopy, the results of which are presented and discussed in the next section.

The structural perfection of the sample becomes particularly evident when examining dynamical diffraction effects. In Fig. 6 we present the theoretical and experimental diffraction patterns very close to the (a) (400) and (b) (422) reflection. The complex interference structure

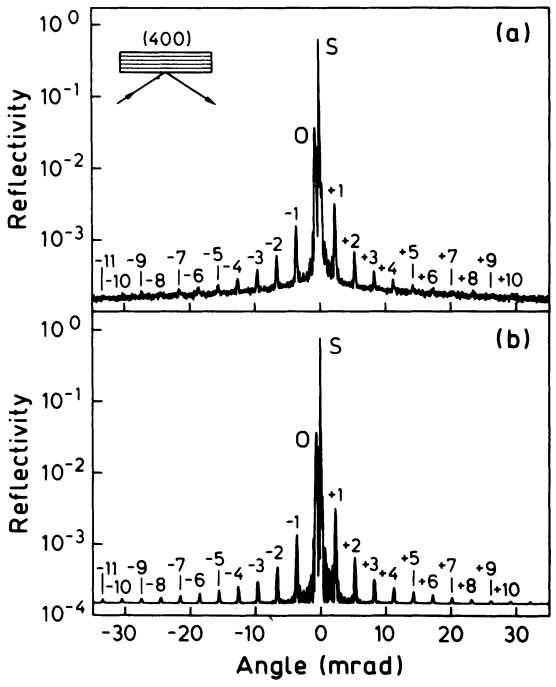

FIG. 4. (a) Experimental and (b) simulated x-ray diffraction pattern in the vicinity of the symmetrical (400) reflection for an InAs/GaAs multilayer structure consisting of 10 InAs lattice planes with a mean In coverage of 0.8 ML, separated by 31.5-nm GaAs.

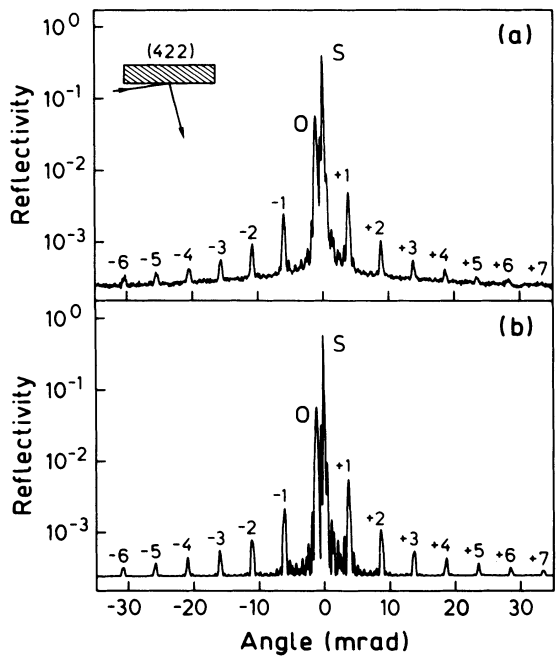

FIG. 5. (a) Experimental and (b) simulated x-ray diffraction pattern in the vicinity of the asymmetrical (422) reflection for the InAs/GaAs multilayer structure of Fig. 4.

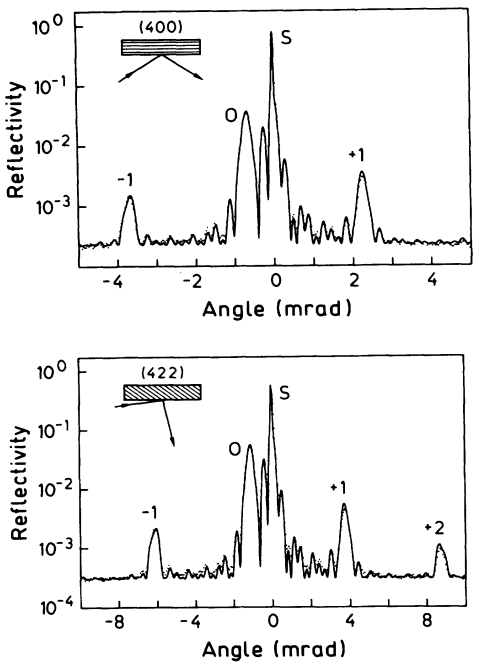

FIG. 6. Details of the diffraction patterns shown in Figs. 4 and 5 very close to the (a) (400) and (b) (422) reflection on an enlarged scale. The complex interference structure around the main reflections originates from the dynamic diffraction of the incident x-ray wave field on the whole heterostructure.

around the main reflections as well as the asymmetric shape of the main reflections are dynamic phenomena, resulting from the interference of phase-coherent x-ray wave fields reflected from the heterointerfaces. The prediction of the dynamical diffraction theory is closely reproduced by the experiment, which demonstrates the perfection of this artificial superlattice. For a more quantitative insight, we have calculated the theoretical diffraction patterns of a superlattice for which each of the 3 ML of the initial GaAs layer contain 10% In (i.e., 3 ML of $In_{0.1}Ga_{0.9}As$). The interference structure is significantly altered from that find in the experiment. In the experimental diffaction patterns of superlattices with a thickness of the initial layer of 7 ML the interference structure is actually damped out. As already discussed in the foregoing section, we take this finding as an indication of residual In in the overgrown layer which was not driven to the surface during the heating cycle. The segregation process is expected to take place preferentially in presence of local inhomogeneities of the crystal, such as surface steps or native defects.[12] The segregation rate is therefore spatially fluctuating, and the composition of the overgrown layer will be locally different. As mentioned above, the composition fluctuation destroys the phase coherence of the x-ray wave fields and consequently inhibits the occurrence of the interference structure. The striking agreement between theory and experiment in Fig. 6 thus provides evidence of the full depletion of the initial GaAs layer.

Next, we present the experiments on the second of the structures mentioned above, composed of a single-layer InAs having a nominal thickness of 3.6 ML (six deposition steps) capped with 200-nm GaAs. The analysis of this structure by HRDXD provides an answer to the question provoked by the RHEED experiments discussed in Sec. IV, namely, whether or not InAs films of this thickness actually remain in the coherently strained state. To address this point, a *single* InAs layer is examined to rule out misleading interpretations related to the overall structural stability of multilayers. The x-ray interference technique provides precise determination of the strain state of even a single monolayer. The lattice distortion of the sandwiched InAs layer breaks the periodicity of the (100) lattice planes in the crystal; i.e., it decouples the lattice of the GaAs cap layer from that of the GaAs substrate. This decoupling leads to a phase shift of the incident x-ray wave field diffracted from both the cap layer and the substrate at identical Bragg angles. An interference phenomenon results which is directly related to the strain state of the embedded layer. Figure 7 shows the symmetrical (400) and asymmetrical (422) diffraction pattern of the structure under consideration. The excellent agreement of the experimental diffraction pattern with the theoretical prediction for a perfect crystal confirms the high degree of interface perfection obtained even for layers close to the critical thickness. Both of the diffraction patterns shown in Fig. 7 are reproduced by the same set of parameters. In particular, an in-plane strain of zero is assumed for the calculation, revealing that the strain is, in fact, entirely accommodated by the elastic tetragonal distortion of the InAs unit cell. The thickness of the embedded InAs film is determined to be 2.4 ML. The difference between the deposited (3.6 ML) and actually incorporated amount of In directly corresponds to

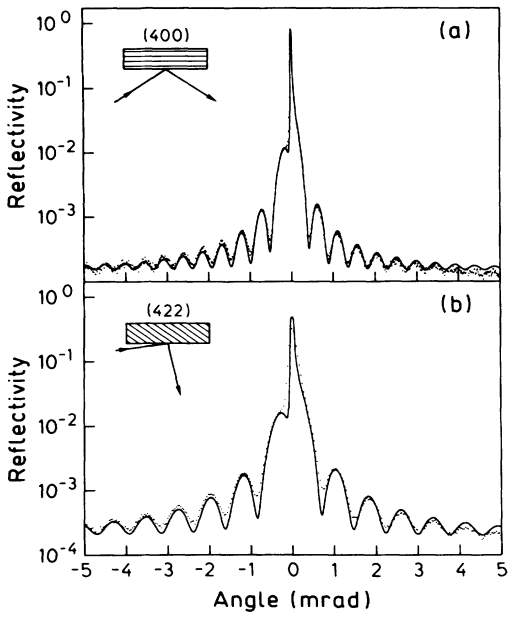

FIG. 7. Experimental (dotted line) and simulated (solid line) diffraction patterns in the vicinity of (a) the symmetrical (400) reflection and (b) the asymmetrical (422) reflection, respectively, for an InAs/GaAs heterostructure consisting of a single InAs layer of 2.4-ML thickness, capped with 200-nm GaAs.

the fraction of In which is lost by the heating cycle, as discussed above. The question arises as to whether or not the film is also in registry with the underlying GaAs lattice *prior to* overgrowth, where it is much thicker. Actually, the amount of segregated In is much higher when strain relief occurs, suggesting that the film tries to stay in registry with the substrate by reducing its thickness. This observation will be discussed in detail in a forthcoming paper.[31]

V. ATOMIC-SCALE MORPHOLOGY OF THE InAs/GaAs HETEROINTERFACES

High-resolution electron microscopy nowadays offers true atomic resolution (point resolution 1.6 Å), and is thus the instrument of choice whenever structural information on an atomic scale is required. In particular, the integral information obtained from x-ray diffraction is complemented by the local probe provided by the focused electron beam. However, high-resolution lattice images of semiconductor heterointerfaces generally show neither the correct position nor the correct thickness of the interface. Reliable quantitative interpretation is complicated by artifacts caused by the mixing of amplitude and phase contrast, by microscope abberations, and by fresnel contrast. In order to obtain lattice images free from those artifacts, the experimental micrographs are processed using a frequency filter. For the determination of the InAs layer thickness in terms of multiples of monolayers, a resolution corresponding to the distance between In-As dumbells parallel to the interface plane (i.e., 0.283 nm) is sufficient. Thus reconstructed lattice images are computed by Fourier filtering with a maximum transferred spatial frequency of 3.4 nm^{-1}. In this way, artifacts due to spherical abberation can be minimized and the InAs layer can be clearly distinguished from the GaAs matrix. Extensive image simulations verify that for sufficient ranges of defocus value (-20 to -50 nm) and specimen thickness (8 to 15 nm) the positions of the dark spots in the reconstructed lattice images directly correspond to the projection of columns of In-As bonds, thus providing accurate quantitative information on the atomic-scale morphology of the interface.[44]

In Fig. 8, we present the high-resolution lattice image of an InAs film with a nominal thickness of 2.4 ML (six deposition steps; see discussion in the preceding section) embedded in the GaAs matrix. The unprocessed micrograph (a) is shown, as well as an enlarged portion of the image obtained after reconstruction (b). On the left of the reconstructed image, the corresponding image simulation for a two-monolayer-thick film is shown. Both of the interfaces are free from defects and appear to be abrupt on an atomic scale. Only a single monolayer step is detected at the upper interface, which connects regions of 2- and 3-ML thickness. The atomic configuration at the interfaces is most evident in the color-coded three-dimensional representation of the experimental (unprocessed) micrograph, as presented in Fig. 9. The same part as that displayed in Fig. 8(b) is shown. Here, the mean intensity of the average unit cell of the GaAs matrix is used as a reference for recognition of the GaAs matrix and the InAs columns. The difference between the mean intensity of a local unit cell and the reference level is translated into the third dimension. The color, in turn, is directly proportional to the respective intensity of the projected columns of the matrix and the InAs layer. Thanks to the chemical sensitivity of the imaging conditions used here, we can distinguish projected GaAs columns and those with an average In content higher than 30%. These experiments are thus less sensitive to interface grading than the x-ray measurements discussed in the preceding section. They demonstrate, however, that both interfaces are of equivalent atomic abruptness. The vertical fluctuation of the interface consists of monoatomic steps with a lateral extent in the nm range. In fact, the microscopic interface configuration of this highly strained system compares favorably with that of GaAs/$Al_xGa_{1-x}As$ heterostructures.[45]

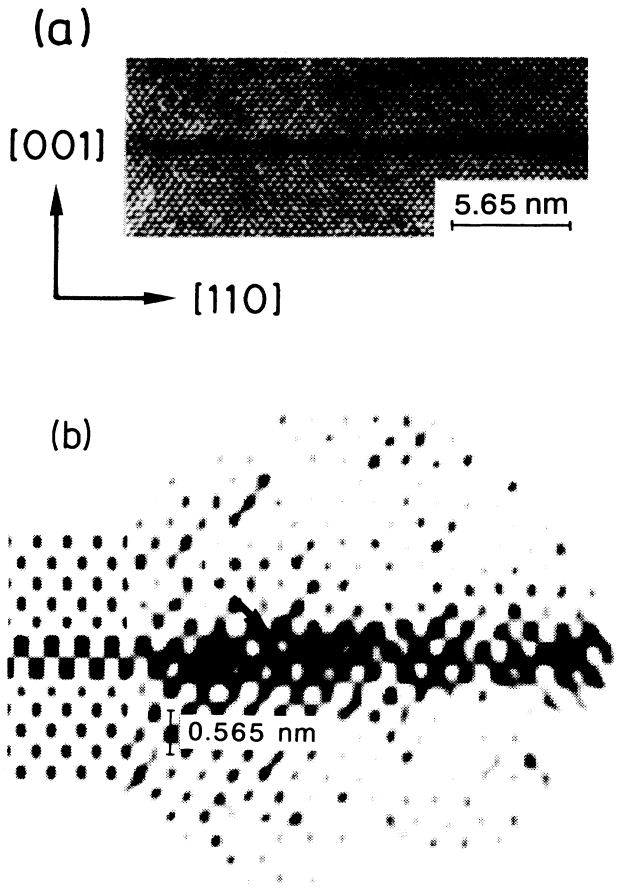

FIG. 8. (a) Lattice image of an InAs/GaAs heterostructure with an InAs thickness of nominally 2.4 ML. (b) Enlarged portion of the micrograph shown in (a) obtained after reconstruction (right) and corresponding image simulation for two InAs monolayers (left). Both images are Fourier filtered for reconstruction allowing maximum spatial frequencies of 3.4 nm^{-1}. The position of the dark spots in the images directly reflects the projection of columns of In-As dumbells. The arrow denotes the position of a single-atomic step connecting regions of 2- and 3-ML thickness.

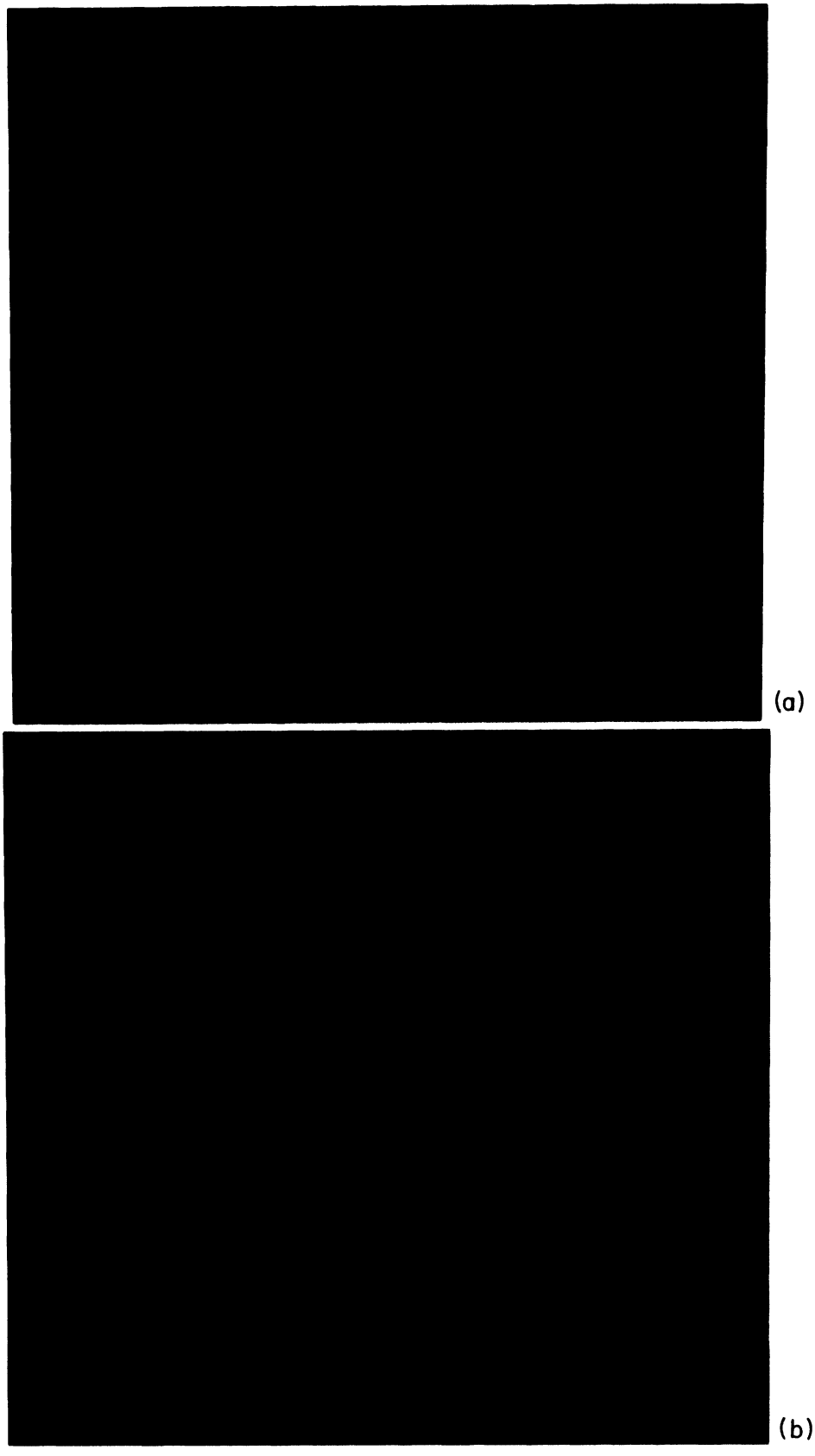

FIG. 9. Color-coded 3D representations of an enlarged portion of the unprocessed experimental image [Fig. 8(a)]. The same part as that shown in Fig. 8(b) is presented. The perspective is chosen to clearly depict (a) the upper and (b) the lower interface, respectively. The rods in the center of the figure correspond to the projected In-As bonds. Both interfaces are structurally equivalent.

VI. CONCLUSIONS

To summarize, we have studied the synthesis of InAs/GaAs heterostructures by conventional solid-source MBE. The fabrication of InAs layers embedded within GaAs requires the controlled buildup of both InAs/GaAs and GaAs/InAs interfaces. In either case, interface formation is dictated by the specific balance of surface and interface energy as well as by kinetic processes during growth. Hence, creating an embedded layer demands, first of all, a detailed understanding of the factors dominating the interface formation, which then represents the basis for the development of strategies to obtain the optimum morphology against thermodynamic and kinetic odds.

The nucleation of InAs on GaAs takes place in the Stranski-Krastanov mode. The film grows layer by layer before the buildup of strain induces the morphological phase transition. Thus wetting of the substrate is energetically favored in this stage of growth. Allowing the surface to relax towards equilibrium consequently minimizes the step density on the growth surface, leading to an atomically smooth InAs film on (001) GaAs. On the other hand, the interplay of surface and interface energy dictates an immediate islanding when depositing GaAs on top of this InAs film. To inhibit formation of the equilibrium configuration, growth-front kinetics is restricted by the rapid (1 ML/s) deposition of a few monolayers of GaAs at low temperature (420 °C). In fact, this strategy prevents island formation and results in a continuous coverage of the surface, serving as basis for further epitaxial deposition under normal growth conditions. However, after low-temperature deposition of 3-ML GaAs, a fraction of the deposited In segregates on the surface. Continuous overgrowth would lead to the incorporation of this In floating layer, dissolving the smooth InAs film into the growing crystal. Stopping the growth and heating to temperatures higher than the desorption point of In on GaAs (500 °C) results in the complete flashoff of the In floating layer prior to overgrowth. Furthermore, this heating cycle establishes the surface-subsurface composition equilibrium, leading to the full depletion of the subsurface region. Any incorporation of segregated In is thus prevented.

The structural configuration of the InAs/GaAs interfaces synthesized by this technique were examined by high-resolution double-crystal x-ray diffraction and high-resolution electron microscopy. Quantitative information on the atomic-scale morphology of the interface was obtained by comparing the experimental results to pattern simulations. Both of the interfaces were shown to be of atomic abruptness, and neither compositional grading nor short-range roughness is present. This fact demonstrates the unique capability of molecular-beam epitaxy in controlling both thermodynamics and kinetics of crystal growth on an atomic scale. Exploitation of this capability opens up promising possibilities in creating artificial materials with desired electronic and optical properties.

ACKNOWLEDGMENTS

We are indebted to A. Fischer for his active contribution to MBE growth. We thank G. Crook and L. Däweritz for valuable discussion of RHEED data, C. Lange for performing scanning electron microscopy measurements, and M. Kelsch for preparation of the HREM samples. This work was supported by the Bundesministerium für Forschung und Technologie of the Federal Republic of Germany.

*Present address: Technische Hochschule Darmstadt, Fachbereich für Materialwissenschaften, D-6100 Darmstadt, Germany.

†Present address: Centro Nazionale Ricerca e Sviluppo Materiali (CNRSM), I-72023 Mesagne, Italy.

[1]K. Ploog, Angew. Chem. Int. Ed. Engl. **27**, 593 (1988).

[2]E. G. Bauer, B. W. Dodson, D. J. Ehrlich, L. C. Feldman, C. P. Flynn, M. W. Geis, J. P. Harbison, R. J. Matyi, P. S. Peercy, P. M. Petroff, J. M. Phillips, G. B. Stringfellow, and A. Zangwil, J. Mater. Res. **5**, 852 (1990).

[3]T. Sands, C. J. Palmstrøm, J. P. Harbison, V. G. Keramidas, N. Tabatabaie, T. L. Cheeks, R. Ramesh, and Y. Silberberg, Mater. Sci. Rep. **5**, 99 (1990).

[4]E. Bauer, Z. Kristallogr. **110**, 372 (1958).

[5]S. M. Pintus, S. I. Stenin, A. I. Toporov, E. M. Trukhanov, and V. Y. Karasyov, Thin Solid Films **151**, 275 (1987).

[6]M. Copel, M. C. Reuter, E. Kaxiras, and R. M. Tromp, Phys. Rev. Lett. **63**, 632 (1989).

[7]D. J. Eaglesham and M. Cerullo, Phys. Rev. Lett. **64**, 1943 (1990).

[8]J. W. Matthews, D. C. Jackson, and A. Chambers, Thin Solid Films **26**, 129 (1975).

[9]W. J. Schaffer, M. D. Lind, S. P. Kovalczyk, and R. W. Grant, J. Vac. Sci. Technol. B **1**, 688 (1983).

[10]F. Houzay, C. Guille, J. M. Moison, P. Henoc, and F. Barthe, J. Cryst. Growth **81**, 67 (1987).

[11]C. Guille, F. Houzay, J. M. Moison, and F. Barthe, Surf. Sci. **189/190**, 1041 (1987).

[12]J. M. Moison, C. Guille, F. Houzay, F. Barthe, and M. Van Rompany, Phys. Rev. B **40**, 6149 (1989).

[13]F. D. Schowengerdt, F. J. Grunthaner, and J. K. Liu, in *Advances in Materials, Processing and Devices in III-V Compound Semiconductors,* MRS Symposia Proceedings No. 144 (Materials Research Society, Pittsburgh, 1989), p. 201.

[14]S. V. Ivanov, P. S. Kop'ev, and N. N. Ledentsov, J. Cryst. Growth **104**, 345 (1990).

[15]J. M. Gérard and J. Y. Marzin, Appl. Phys. Lett. **53**, 568 (1988); J. M. Gérard, J. Y. Marzin, B. Jusserand, F. Glas, and J. Primot, *ibid.* **54**, 30 (1989).

[16]J. M. Moison, F. Houzay, F. Barthe, J. M. Gérard, B. Jusserand, J. Massies, and F. S. Turco-Sandroff, J. Cryst. Growth **111**, 141 (1991).

[17]A. J. SpringThorpe, S. J. Ingrey, B. Emmerstorfer, and P. Mandelville, Appl. Phys. Lett. **50**, 77 (1987).

[18]T. Mizutani, J. Vac. Sci. Technol. B **6**, 1671 (1988).

[19]L. Däweritz, Superlatt. Microstruct. **9**, 141 (1991).

[20]B. F. Lewis, R. Fernandez, A. Madhukar, and F. J. Grunthaner, J. Vac. Sci. Technol. B **4**, 560 (1986).
[21]O. Brandt, L. Tapfer, R. Cingolani, K. Ploog, M. Hohenstein, and F. Phillipp, Phys. Rev. B **41**, 12 599 (1990).
[22]L. Tapfer and K. Ploog, Phys. Rev. B **33**, 5565 (1986).
[23]J. H. Neave, B. A. Joyce, and P. J. Dobson, Appl. Phys. A **34**, 179 (1984).
[24]P. K. Larsen and D. J. Chadi, Phys. Rev. B **37**, 8282 (1988).
[25]P. K. Larsen, J. H. Neave, J. F. van der Veen, P. J. Dobson, and B. A. Joyce, Phys. Rev. B **27**, 4966 (1983).
[26]H. H. Farrell and C. J. Palmstrøm, J. Vac. Sci. Technol. B **8**, 903 (1990).
[27]J. M. Moison, C. Guille, and M. Bensoussan, Phys. Rev. Lett. **58**, 2555 (1987).
[28]J. H. Neave, B. A. Joyce, P. J. Dobson, and N. Norton, Appl. Phys. A **31**, 1 (1983).
[29]B. F. Lewis, F. J. Grunthaner, A. Madhukar, T. C. Lee, and R. Fernandez, J. Vac. Sci. Technol. B **3**, 1317 (1985).
[30]L. Däweritz, J. Griesche, R. Hey, and J. Herzog, J. Cryst. Growth **111**, 65 (1991).
[31]L. Tapfer, O. Brandt, K. Ploog, M. Hohenstein, and F. Phillipp (unpublished).
[32]F. J. Grunthaner, M. Y. Yen, R. Fernandez, T. C. Lee, A. Madhukar, and B. F. Lewis, Appl. Phys. Lett. **46**, 983 (1985).
[33]A. Madhukar, T. C. Lee, M. Y. Yen, P. Chen, J. Y. Kim, S. V. Ghaisas, and P. G. Newman, Appl. Phys. Lett. **46**, 1148 (1985).
[34]R. A. Stall, J. Zilko, V. Swaminathan, and N. Schumaker, J. Vac. Sci. Technol. B **3**, 524 (1985).
[35]L. Däweritz and R. Hey, Surf. Sci. **236**, 15 (1990).
[36]J. A. McCaulley and V. M. Donelly, J. Chem. Phys. **91**, 4330 (1989).
[37]H. Yamaguchi and Y. Horikoshi, J. Appl. Phys. **68**, 1610 (1990).
[38]L. Tapfer, Phys. Scr. T **25**, 45 (1989).
[39]L. Tapfer, N. Kobayashi, T. Makimoto, and Y. Horikoshi, J. Phys. C **5**, 521 (1987).
[40]J. M. Vandenberg, M. B. Panish, R. A. Hamm, and H. Temkin, Appl. Phys. Lett. **56**, 910 (1990).
[41]L. Tapfer and K. Ploog, Phys. Rev. B **40**, 9802 (1989).
[42]L. Tapfer, M. Ospelt and H. von Känel, J. Appl. Phys. **67**, 1298 (1990).
[43]H. Holloway, J. Appl. Phys. **67**, 6229 (1990).
[44]M. Hohenstein, F. Phillipp, O. Brandt, L. Tapfer, and K. Ploog, in *Proceedings of the Seventh Oxford Conference on Microscopy of Semiconducting Materials, London, 1991,* Inst. Phys. Conf. Ser. No 117 (Institute of Physics and Physical Society, Bristol, 1991) p. 611.
[45]A. Ourmazd, W. T. Tsang, J. A. Rentschler, and D. W. Taylor, Appl. Phys. Lett. **50**, 1417 (1987); A. Ourmazd, J. Cryst. Growth **98**, 72 (1989).

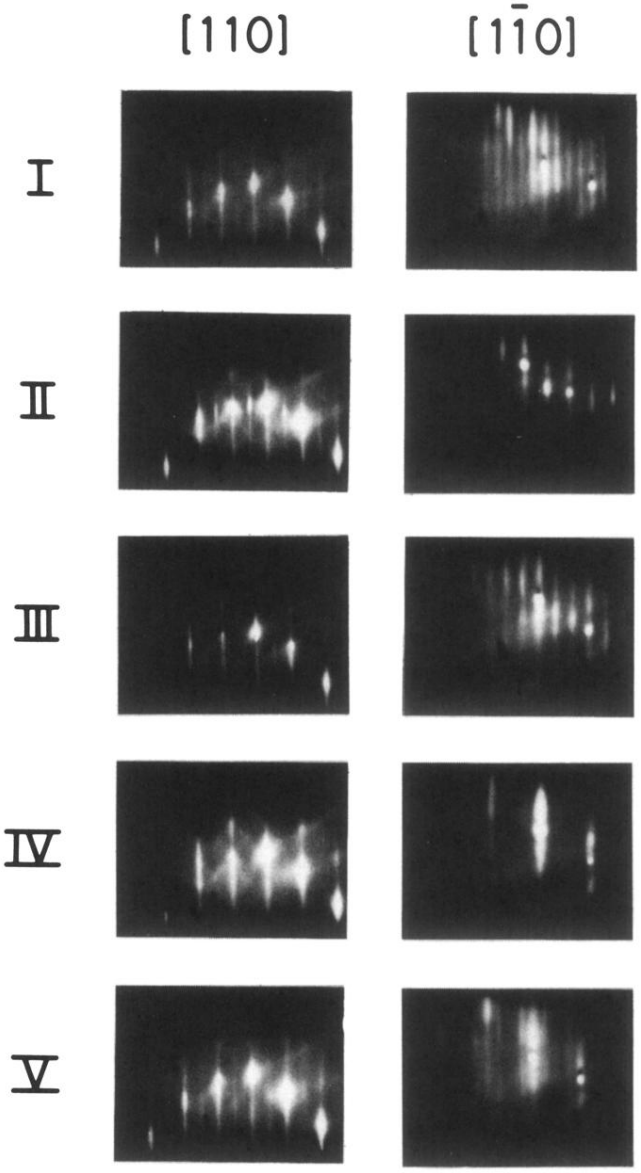

FIG. 2. RHEED patterns taken during the deposition of 1.2-ML InAs on GaAs and the subsequent overgrowth with GaAs. Roman numbers refer to Fig. 1. The azimuth of the incident electron beam is denoted on the top. (I) (2×4) reconstruction of the dynamic (growing) GaAs surface at 540 °C, (II) $c(4\times4)$ reconstruction of the static (nongrowing) GaAs surface at 440 °C, (III) (2×3) As-stable reconstruction of the static InAs surface after deposition of $\simeq$1.2-ML InAs at 420 °C, (IV) (1×1) reconstruction of the static surface after deposition of $\simeq$3-ML GaAs at 420 °C on top of the InAs monolayer, (V) $(2\times4)_\gamma$ reconstruction of the same (static) surface at 520 °C.

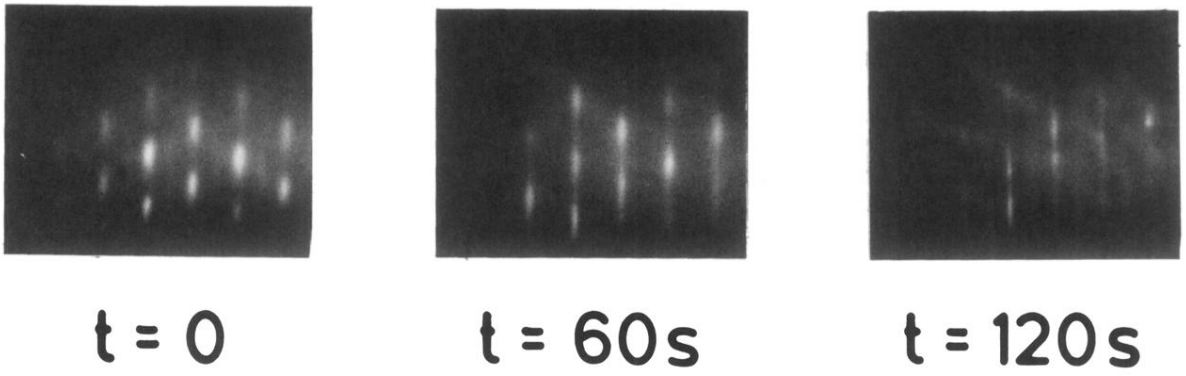

FIG. 3. RHEED patterns of the relaxing InAs surface taken along the [110] azimuth after the deposition of 3.6-ML InAs (six deposition steps) on GaAs at 420 °C. The time indicated at the respective pattern corresponds to the annealing time after closing the In shutter.

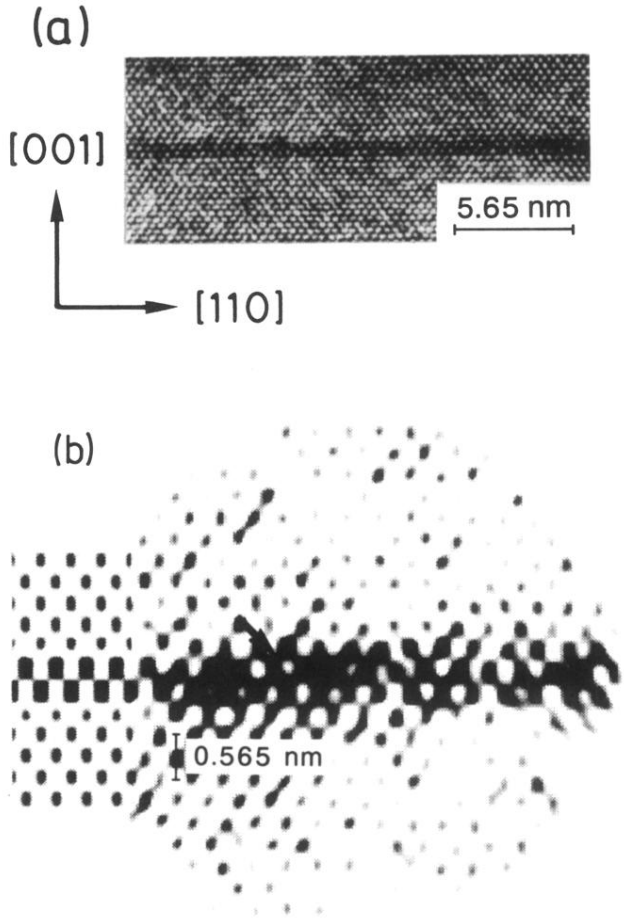

FIG. 8. (a) Lattice image of an InAs/GaAs heterostructure with an InAs thickness of nominally 2.4 ML. (b) Enlarged portion of the micrograph shown in (a) obtained after reconstruction (right) and corresponding image simulation for two InAs monolayers (left). Both images are Fourier filtered for reconstruction allowing maximum spatial frequencies of 3.4 nm^{-1}. The position of the dark spots in the images directly reflects the projection of columns of In-As dumbells. The arrow denotes the position of a single-atomic step connecting regions of 2- and 3-ML thickness.

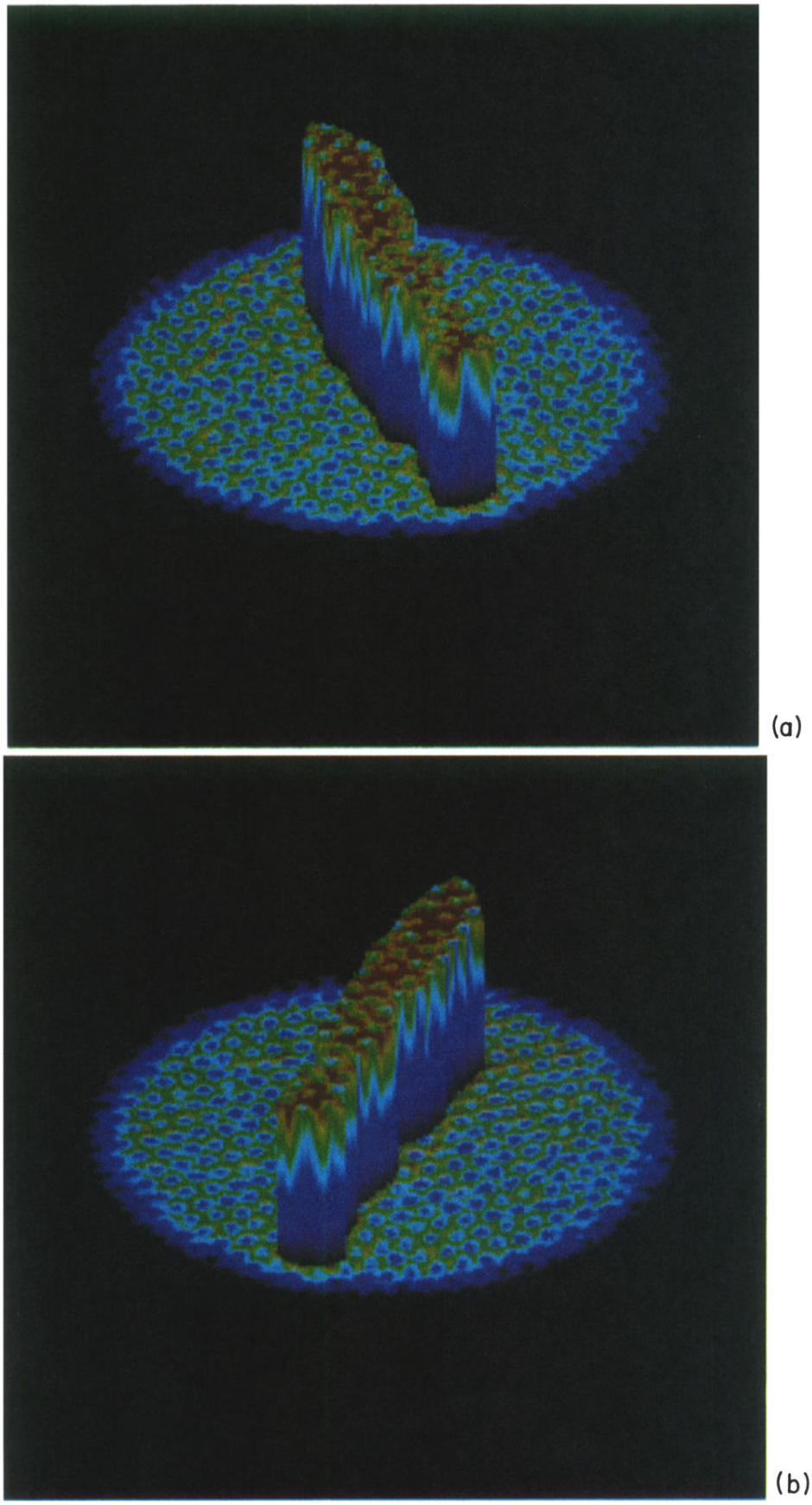

FIG. 9. Color-coded 3D representations of an enlarged portion of the unprocessed experimental image [Fig. 8(a)]. The same part as that shown in Fig. 8(b) is presented. The perspective is chosen to clearly depict (a) the upper and (b) the lower interface, respectively. The rods in the center of the figure correspond to the projected In-As bonds. Both interfaces are structurally equivalent.